Electrochemistry Communications 121 (2020) 106852

Contents lists available at ScienceDirect

Electrochemistry Communications

journal homepage: www.elsevier.com/locate/elecom

Nitrofluorene derivatives trapped within MWCNTs for electrocatalysis of NADH: Substituent effects on π-π stacking interaction strength

J. Urzúa[a], C. Yañez[a], J. Carbajo[b], J.D. Mozo[b], J.A. Squella[a,*]

[a] Centro de Investigación de los Procesos Redox (CIPRex), Facultad de Ciencias Químicas y Farmacéuticas, Universidad de Chile, Santiago, Chile
[b] Centro de Investigación Científico Tecnológico de Huelva: Departamento de Electroquímica Aplicada, Universidad de Huelva, Huelva, Spain

ARTICLE INFO

Keywords:
Nitrofluorene derivatives
MWCNT
NADH
Carbon nanotube
Catalytic
Electrooxidation

ABSTRACT

We describe nanostructured electrode platforms composed of multiwalled carbon nanotube/glassy carbon electrodes (MWCNT/GCEs) with entrapped nitroaromatic compounds such as 2-nitrofluorene (2-NF), 2-nitro-9-fluorenone (2-NFN), 2,7-dinitrofluorene (2,7-NF) and 2,7-dinitro-9-fluorenone (2,7-NFN). All of the above nitroaromatic compounds were tested as precursors for the production of redox mediator couples useful for NADH electrocatalysis.

In this communication, we reveal the effect of the substituents on both the π-π stacking interaction strength and the electrocatalysis of NADH.

The results show that the nitro group plays a triple role: it acts as a precursor of the mediator redox couple for NADH electrocatalysis; it increases the π-π stacking interaction with the electrode; and it acts as an electron acceptor substituent that promotes the electrocatalysis of NADH.

1. Introduction

The discovery of carbon nanotubes (CNTs) started a revolution in electrode materials. The most cited paper is a report by Ijima et al. in 1991 [1]; however, the existence of CNTs was known well before that date [2]. The bonding in CNTs is essentially based on sp^2 hybridization, however, the tube curvature, as well as giving rise to quantum confinement and quantized conductance, also causes σ–π rehybridization; this effect becomes stronger with decreasing CNT diameter [3]. In this case, three σ bonds are slightly out of plane and to compensate, the π orbitals are more delocalized outside the tube. This is the main difference between CNTs and graphite, in which the sp^2 hybrid orbital forms three in-plane σ bonds with an out-of-plane π orbital. The electron cloud distortion induced by tube curvature yields a rich π-electron conjugation outside the tube which makes CNTs more electrochemically active and more electrically and thermally conductive. This is key to the success of CNTs as an electrode material. The high specific surface area of CNTs together with the σ–π rehybridization and the presence of structural defects facilitate a range of chemical processes such as chemical derivatization, intercalation, molecular adsorption, doping, and charge transfer [4,5]. One of the most important advantages of CNTs is the possibility of modifying them with various organic or inorganic chemical compounds that dramatically change the properties of the electrode phase. These modifications can be carried out using either covalent [6–8] or non-covalent (physisorption) [9,10] attachment of the modifier to the three-dimensional array of CNTs.

Physical adsorption of small molecules is a promising approach to functionalizing CNTs. Physical functionalization enhances dispersibility and preserves the extended π networks of the CNTs. This type of functionalization can be achieved in several different ways, including π-π stacking interactions and electrostatic interactions. Physical functionalization of CNTs by π-π stacking interactions, in which the π electrons on the CNT surface interact with the π electrons of small molecules, is one of the most important approaches.

Several studies have demonstrated the modification of CNTs with nitroaromatics using the covalent attachment of the nitroaromatic group to the CNTs [11–15]. However, we have recently revealed a different strategy for the modification of CNTs with nitroaromatics that does not involve covalent attachment [16–19]. This strategy is based on trapping nitroaromatics within pockets on the surface of the three-dimensional array of MWCNTs.

The search for new nitroaromatics with strategic functional groups that can be trapped on MWCNTs in this way has been an objective of our research in recent years because direct immobilization of redox mediators on the carbon surface is an elegant approach to tailoring the electrode surface. In this research effort, we have shown that it is possible to obtain electrodes with better characteristics than a bare GCE

* Corresponding author.
E-mail address: asquella@ciq.uchile.cl (J.A. Squella).

https://doi.org/10.1016/j.elecom.2020.106852
Received 24 September 2020; Received in revised form 9 October 2020; Accepted 11 October 2020
Available online 15 October 2020

by the appropriate modification of a GCE with MWNCTs and the subsequent trapping of nitroaromatics.

We have previously studied the electrochemical behaviour of entrapped 2,7-dinitro-9-fluorenone (2,7-NFN) on a MWCNT/GCE and compared it with the adsorption at a bare GCE previously reported by Mano et al. [20]. In this work, we are interested in studying the substituent effect of entrapped nitrofluorene and nitrofluorenone compounds on electrochemical behaviour and evaluate the resulting electrocatalytic activity towards NADH oxidation.

2. Experimental

2.1. Reagents and apparatus

Nitroaromatic compounds: 2-nitrofluorene (2-NF), 2-nitro-9-fluorenone (2-NFN), 2,7-dinitrofluorene (2,7-NF) and 2,7-dinitro-9-fluorenone (2,7-NFN) (Fig. 1) were supplied by Sigma-Aldrich® and used without further purification. All of the other reagents were of analytical grade. Multiwalled carbon nanotubes (MWCNTs, 10 nm in diameter and 1.5 μm in length) were purchased from Dropsens S.L., Spain. Stock solutions of nitroaromatics were prepared in ethanol. A 0.1 M phosphate buffer solution (PBS) (22.83 g of K_2HPO_4 and 13.81 g of KH_2PO_4 in 1 L of ultrapure water) with the pH adjusted to 7.0 using concentrated HCl was used as the supporting electrolyte in all of the measurements except the study of pH dependence. For this latter purpose, a 0.1 M Britton-Robinson buffer (6.18 g of H_3BO_3, 5.7 mL of CH_3COOH and 6.74 mL of H_3PO_4 in 1 L of ultrapure water) was used. Ultrapure water was obtained from the Merck Millipore Milli-Q® Reference System. The pH in each case was adjusted using concentrated solutions of either HCl or NaOH.

Electrochemical measurements (cyclic voltammetry, CV) were carried out using a BASi 100 voltammetric analyser (BASi Analytical Instruments, USA). A CHI 650C potentiostat (CH Instruments Inc., USA) was also employed. A conventional 3-electrode system was used with a nitro-modified glassy carbon electrode (GCE) 3 mm in diameter (model CHI104, CH Instruments) as the working electrode. Ag/AgCl/3M NaCl (BASi MF-2052) and a Pt wire were used as the reference and counter electrodes, respectively.

2.2. Preparation of MWCNT/GCEs

MWCNT/GCEs were prepared following the procedure described in a previous report [21].

2.3. Trapping nitrofluorene derivatives in the MWCNT/GCE

MWCNT/GCEs were immersed in a 0.1 mM solution of a nitrofluorene derivative dissolved in ethanol for a given time (accumulation time, t_{ac}). The electrodes were then washed with water. The accumulation time and nitrocompound concentration were optimized (see the Supplementary material).

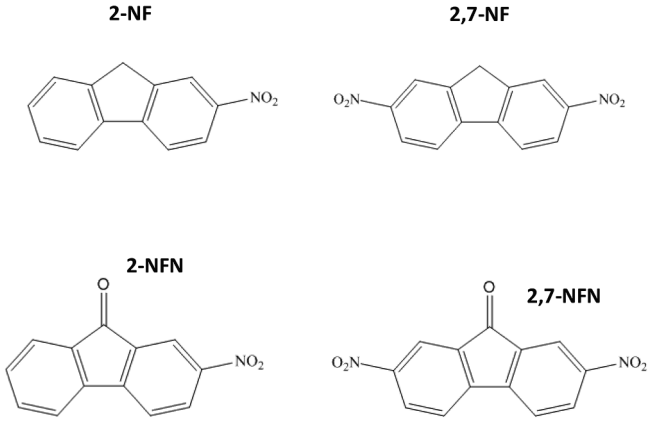

Fig. 1. Chemical structure of 2-nitrofluorene (2-NF), 2,7-dinitrofluorene (2,7-NF), 2-nitro-9-fluorenone (2-NFN) and 2,7-dinitro-9-fluorenone (2,7-NFN).

2.4. Voltammetric measurements

The nitro-functionalized electrodes were immersed in an electrochemical cell containing only the supporting electrolyte (without nitrofluorene derivatives in solution). All of the electrochemical measurements were performed after purging N_2 into the cell solution for 10 min. Experiments were carried out at room temperature (25 ± 1 °C).

To evaluate the electrocatalytic activity of the mediator electrode for NADH, the nitro-functionalized electrode was immersed in an electrochemical cell containing 0.1 M PBS, pH 7.0, and 0.2 mM NADH. The potential was then scanned between −250 and 500 mV vs. Ag/AgCl to record the voltammetric curve.

2.5. Scanning electron microscopy (SEM)

SEM images of the modified electrodes were obtained using an Inspect Scanning Electron Microscope F-50 operated at 20 kV. Glassy carbon discs (TED Pella brand, INC (N 16524)) measuring 12.7 mm in diameter were used.

3. Results and discussion

3.1. Electrochemical behaviour of entrapped nitrofluorene and nitrofluorenone compounds on MWCNT/GCEs

We have previously studied the electrochemical behaviour of some nitroaromatic compounds trapped within the MWCNT array [18,19,22] and the electrocatalytic activity of some of these compounds containing two nitro groups in the oxidation of NADH [18,19]. In this study, we investigate how structural changes in the trapped molecule can affect the electrochemical behaviour.

Fig. 2 displays the cyclic voltammograms of entrapped nitroaromatic compounds on the MWCNT/GCE electrodes at 100 mV s^{-1}. In the first scan (initiated at −240 mV, solid line), the compounds with only one nitro group, namely 2-NF and 2-NFN (Fig. 2A and C, respectively) show an irreversible reduction corresponding to the reductive transformation of the nitro group into a hydroxylamine derivative (peak 1). In the reverse scan, oxidation of the hydroxylamine derivative into a nitroso derivative occurred (peak 4). In the second scan (dotted line), a cathodic peak corresponding to the reduction of the nitroso group to a hydroxylamine derivative appears (peak 4′). Moreover, in this second scan, the nitro reduction peak disappears almost entirely, indicating the depletion of the nitroaromatic compound trapped in the electrode. The peak potential of the nitro reduction and R-NHOH/R-NO redox couple are shifted to more positive potentials due to the presence of the carbonyl group (Fig. 2C). The peak potentials are summarized in Table 1. By contrast, the 2,7-NF and 2,7-NFN dinitro-compounds (Fig. 2B and D, respectively) show two irreversible reduction peaks in the first reduction scan (peaks 1 and 2) corresponding to the two nitro groups present in the molecule forming hydroxylamine derivatives that are subsequently oxidized to nitroso derivatives (peaks 3 and 4 in the oxidation reverse scan). The nitroso derivatives are reduced in the second reduction scan (peaks 3′ and 4′, dotted line) to the corresponding hydroxylamine derivatives. The two redox couples corresponding to R-NHOH/R-NO are denoted as peaks 3/3′ and 4/4′. The peak potentials (*E*p) are also summarized in Table 1. A gradual shift in the peaks towards more positive potentials is observed with the incorporation of $-NO_2$ and −C═O substituents due to the increasing negative inductive effect.

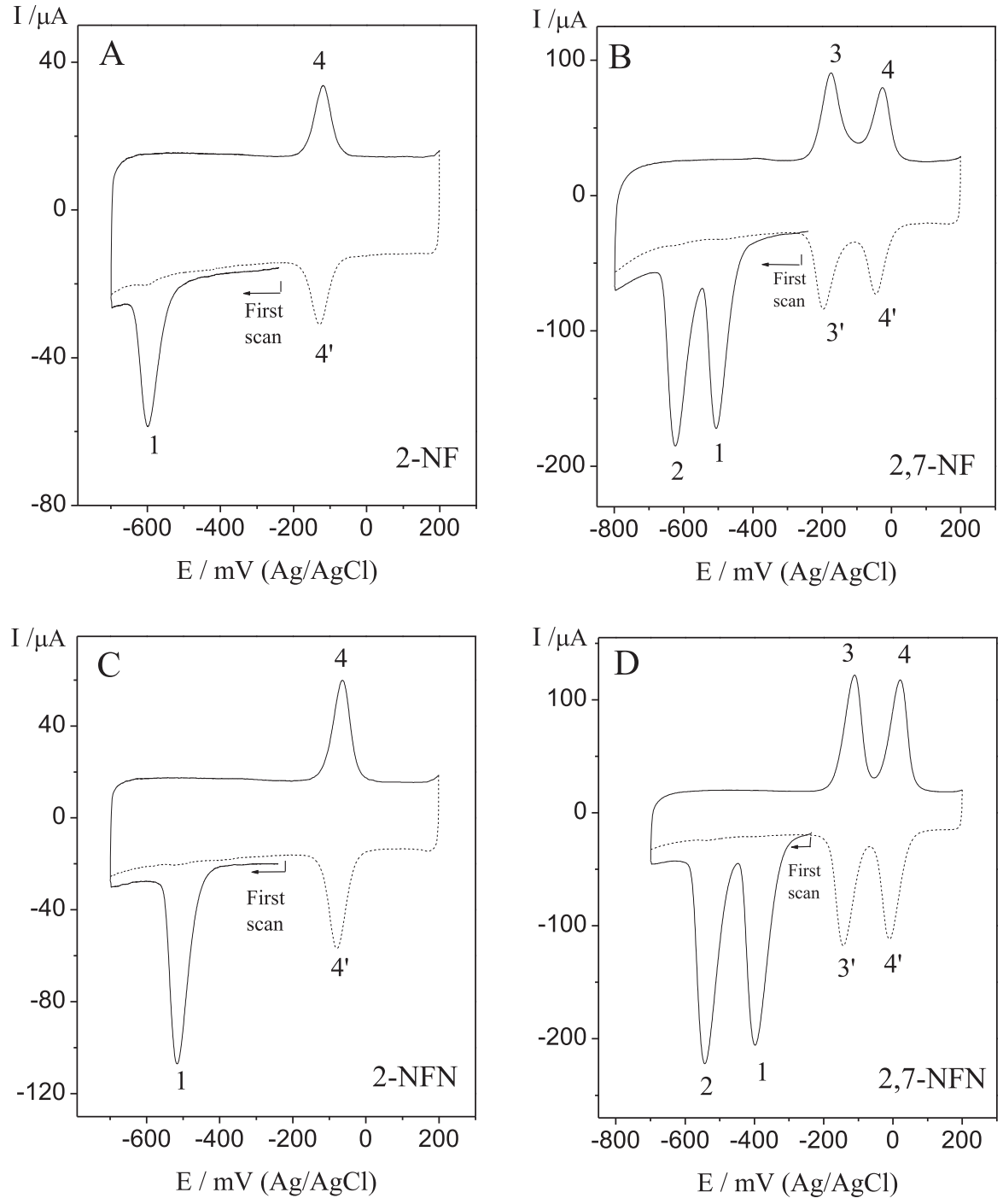

Fig. 2. Cyclic voltammograms of 0.1 mM of (A) 2-NF, (B) 2,7-NF, (C) 2-NFN, and (D) 2,7-NFN trapped in MWCNT/GCE by dipping the electrode in a 0.1 mM nitroaromatic compound in ethanol. Accumulation time: 1 min. CVs registered in 0.1 M PBS pH 7.0 (without NF compounds in solution). Scan rate = 100 mV s^{-1}.

Table 1
Peak potentials (*E*p) of the nitro and dinitro compounds.

	*E*p/mV					
Compound	Peak 1	Peak 2	Peak 3	Peak 3′	Peak 4	Peak 4′
2-NF	−598 ± 9	–	–	–	−105 ± 15	−124 ± 5
2-NFN	−518 ± 8	–	–	–	−51 ± 14	−74 ± 7
2,7-NF	−508 ± 10	−625 ± 10	−160 ± 14	−186 ± 11	−37 ± 10	−66 ± 20
2,7-NFN	−397 ± 14	−543 ± 13	−100 ± 10	−137 ± 6	+22 ± 15	−22 ± 18

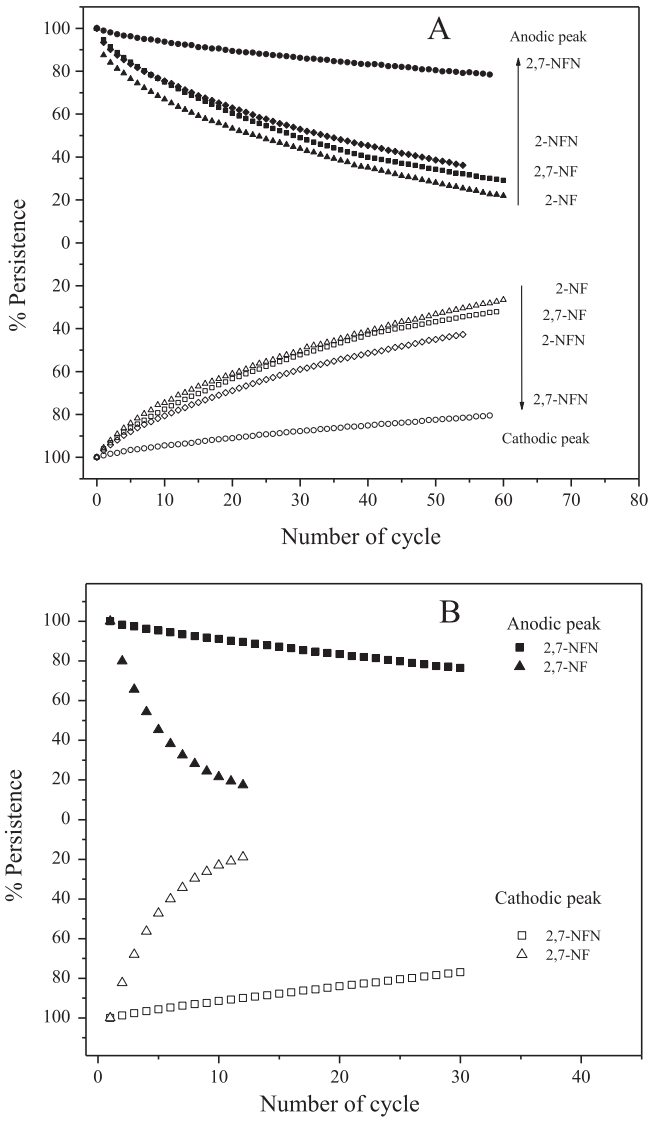

Fig. 3. Evolution of the stability of the redox couple as a function of the number of voltammetric cycles. (A) Reduction of one nitro group per molecule. (B) Reduction of two nitro groups per molecule.

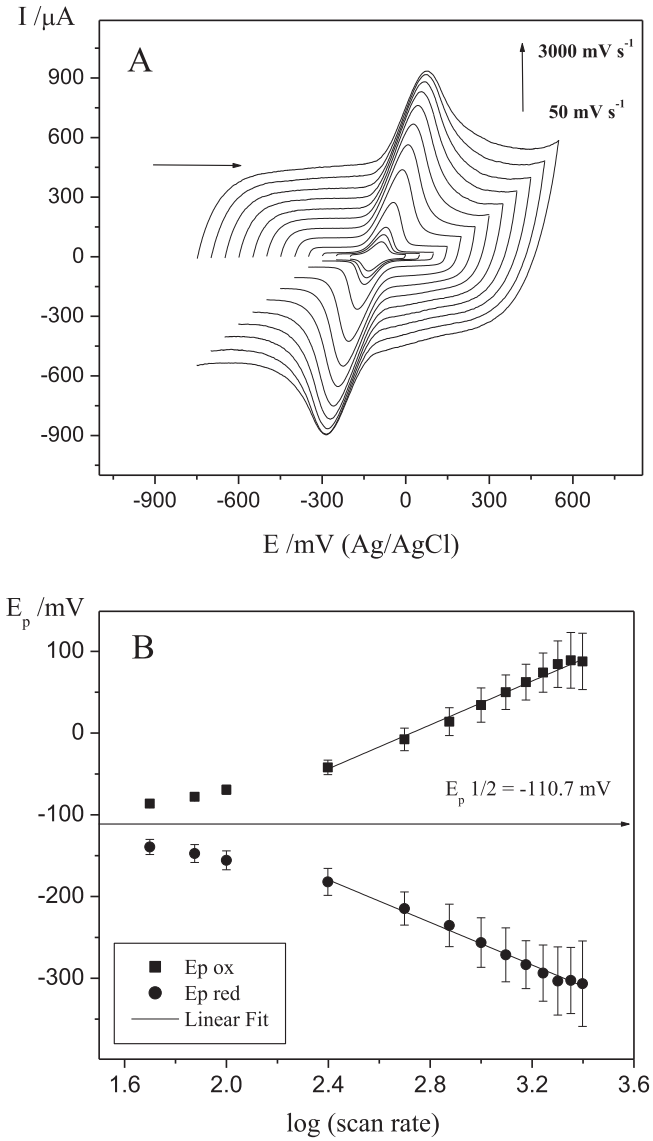

Fig. 4. (A) Cyclic voltammograms of the R-NHOH/R-NO derivative couple of the 2-NF-functionalized MWCNT/GCE in PBS buffer 0.1 M, pH 7.0, recorded at various sweep rates between 50 and 3000 mV s^{-1}. (B) Laviron plot and the corresponding linear regression.

These results show that the overall mechanism for the reactions corresponding to irreversible peaks 1 and 2 can be represented by:

$$RNO_2 + 4H^+ + 4e^- \rightarrow RNHOH + H_2O \quad (1)$$

On the other hand, the overall mechanism for the quasi-reversible redox pairs 3/3′ and 4/4′ can be described by the well-known equation:

$$RNHOH \Leftrightarrow RNO + 2H^+ + 2e^- \quad (2)$$

3.2. Stability of the NHOH/NO redox couple and determination of the heterogeneous constant

The redox pair originating from activation of the nitroaromatic precursor in the MWCNT electrode array remains in the electrode after several potential scans, even though the intensity currents of both anodic and cathodic peaks decrease as the number of cycles increases. We have measured the peak current intensity to characterize the stability of the nitroso and hydroxylamine derivatives in the MWCNT array. To compare the nitro and dinitro compounds, the switching potential was chosen so as to reduce only one nitro group per molecule of the dinitro compounds (2,7-NF and 2,7-NFN). Fig. 3A shows the stability (expressed as a percentage of gradual change in the current intensity and referred to as persistence) as a function of the number of cycles when only one nitro group per molecule was converted into the hydroxylamine derivative. Upon changing the switching potential to reduce two nitro groups, a significant decrease in the current intensity is observed (Fig. 3B).

The persistence results indicate that nitrofluorenes and nitrofluorenones are successfully attached to the MWCNTs in spite of the absence of a covalent bond between the nitroaromatic compounds and the MWCNTs, with 2,7-NFN being the most stable compound in the MWCNT array. These results strongly suggest that substituents with two nitro groups and one C=O group have a strong influence on the π-π stacking strength, indicating a direct interaction between the substituents and another aromatic ring in the MWCNTs. Furthermore, considering the difference observed between the results obtained for the reduction of one or two nitro groups per molecule, we can conclude that the nitro group has a strong effect on the strength of the π-π stacking interaction.

The RNHOH/RNO redox couples were studied at various sweep

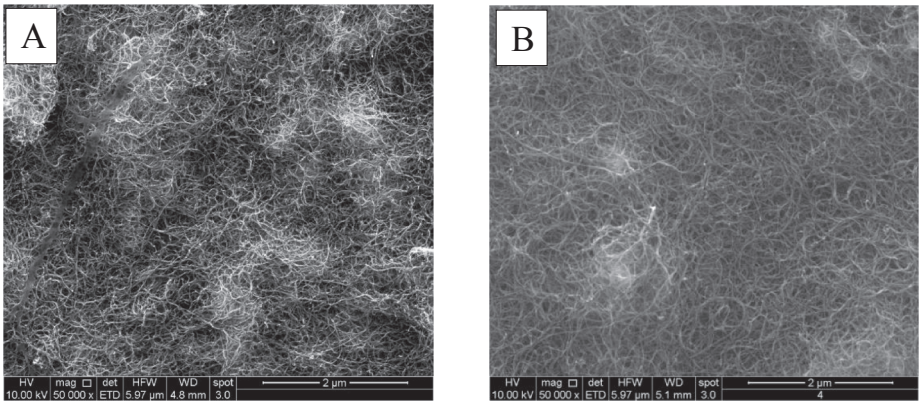

Fig. 5. SEM images of (A) MWCNT/GCE and (B) MWCNT/GCE-2,7-NFN with two nitro groups reduced, where the mediator has also been generated. Magnification ×50,000.

rates (50–3000 mVs^{-1}). The peak currents were proportional to the sweep rate in all of the cases and the relationship between *E*p and log scan rate was evaluated for the anodic and cathodic peaks. An example is shown in Fig. 4 for 2-NF trapped in MWCNT/GCE. Following the procedure previously established for 3,5-dinitrobenzoic acid and the 3,5-dinitrobenzoate derivatives [21,22], the heterogeneous electron transfer rate constants (k_h) were obtained. The resulting values are summarized in Table S1 (in the Supplementary Information). These results indicate that 2,7-NFN is the best candidate for catalysis of NADH. It is important to note that the data do not converge at low scan rates (Fig. 4B). This dispersion of the data is probably due to the fact that the trapped molecules do not all exist in an identical state. Furthermore, other factors such as interactions between molecules and uncompensated resistance could be involved.

As in our previous studies [18,19,22], the shape of the MWCNTs on the GCE before and after the electrochemical procedures has been investigated through SEM imaging. As shown in Fig. 5, the trapping of the nitrocompounds and the derivatives generated after potential scanning do not affect the morphology of the surface.

3.3. Electrocatalytic activity for NADH oxidation

The electrochemical behaviour of all the nitrofluorene and nitrofluorenone compounds was tested in the presence of NADH. The results are shown in Fig. 6. The cyclic voltammogram of NADH on MWCNT/GCE displays a single anodic peak at 260 mV and is shown by the dot-dashed line throughout this figure. The electrochemical behaviour of the corresponding mediator redox couple is shown (as a dashed line) in a similar manner for comparison. The reaction corresponding to the anodic peak of NADH can be represented by:

$$NADH \rightarrow NAD^+ + H^+ + 2e^- \quad (3)$$

When 2-NF/MWCNT/GCE was used, no catalytic current was observed (Fig. 6A). The redox couple 4/4′ of this mediator is the most negative, appearing at −105/−124 mV (Table 1). For 2-NFN/MWCNT/GCE, a broad oxidation charge is observed (Fig. 6C). Apparently, this response is due to the contributions of different oxidation signals. Using the oxidation potential of the redox mediator (−40 mV, Fig. 6C) and NADH, the electrochemical response was deconvoluted using least-squares peak-fitting software (Origin software). The deconvolution of the electrochemical behaviour was fitted into the following contributions from three oxidation processes (inset in Fig. 6C): (i) oxidation of the mediator at −39 mV generating R-NO; (ii) catalysed oxidation of NADH centred at 60 mV; and (iii) non-catalysed oxidation close to 260 mV. The fitted curve shows excellent agreement with the experimental data. The calculated total charge of these two oxidation contributions (92.3 μC) is close to the corresponding oxidation charge of NADH on MWCNT/GCE (90.4 μC). It is important to note that even though the electrode modification procedure was strictly followed, variations of less than 10% can be obtained for the modified electrodes. Therefore, the introduction of the −C═O substituent provides catalytic properties towards NADH oxidation, even though catalysed NADH was still absent.

It was also found that when the 2,7-NF and 2,7-NFN dinitroaromatic compounds were used as the redox precursors and only one nitro group was reduced to hydroxylamine, the oxidation of NADH also shifted to lower positive potentials.

For 2,7-NF/MWCNT/GCE, where the formation of R-NO (peak 4) appeared at −45 mV (Fig. 6B), the *E*p of NADH oxidation shifted from 260 to 70 mV, similar to the change obtained for 2-NFN/MWCNT/GCE (Fig. 6C). However, in this case, according to the deconvoluted curves (inset of Fig. 6B), a very small contribution of uncatalysed NADH may be present at potentials close to 260 mV. The introduction of a second nitro group that exerts an electron-withdrawing effect causes a decrease in the formal potential of the R-NHOH/R-NO redox couple, showing electrocatalytic activity for NADH oxidation.

The most extreme change is observed for 2,7-NFN/MWCNT/GCE (Fig. 6D), which shows an increase in the oxidation current at a potential of 20 mV, near to the formal potential of the R-NHOH/R-NO redox couple, and the complete disappearance of the original signal of NADH oxidation. The total charge of the oxidation signal centred at 20 mV (154.5 μC) is essentially the same as the sum of the signals corresponding to both the oxidation of the redox mediator on MWCNT/GCE (dashed line, Fig. 6D) and the oxidation of NADH (dot-dashed line, Fig. 6D). These kinds of results have been seen previously by other researchers [14,20,23,24]. It has been postulated that the electrocatalytic mechanism for this type of redox mediator (organic 2 electron-proton acceptor) with NADH involves an intermediate charge transfer complex [25]. Recently, Rębiś et al. [26] also observed the electrocatalytic effect of a redox mediator, recording a decrease in the oxidation potential of NADH in a way that practically coincides with the potential of the mediator: NADH is oxidized by the mediator at the electrode; the reduced form of the mediator is electrochemically re-oxidized. Therefore, the oxidation peak current at this potential significantly increases. Our results for 2,7-NFN/MWCNT/GCE are compatible with this proposed mechanism.

Thus, the presence of both nitro groups and −C═O substituents leads to an improved catalytic property towards NADH oxidation. In fact, the electronic effects of the nitro group and −C═O substituents trigger a decrease in the energy requirements of the redox mediator couple, facilitating the oxidation of NADH. Furthermore, substitution with two nitro groups and a single C═O group strongly affects the π-π stacking strength, leading to greater stability of the redox mediator couple on the electrode and favouring electrocatalysis.

Based on the results obtained for these four nitro compounds, when

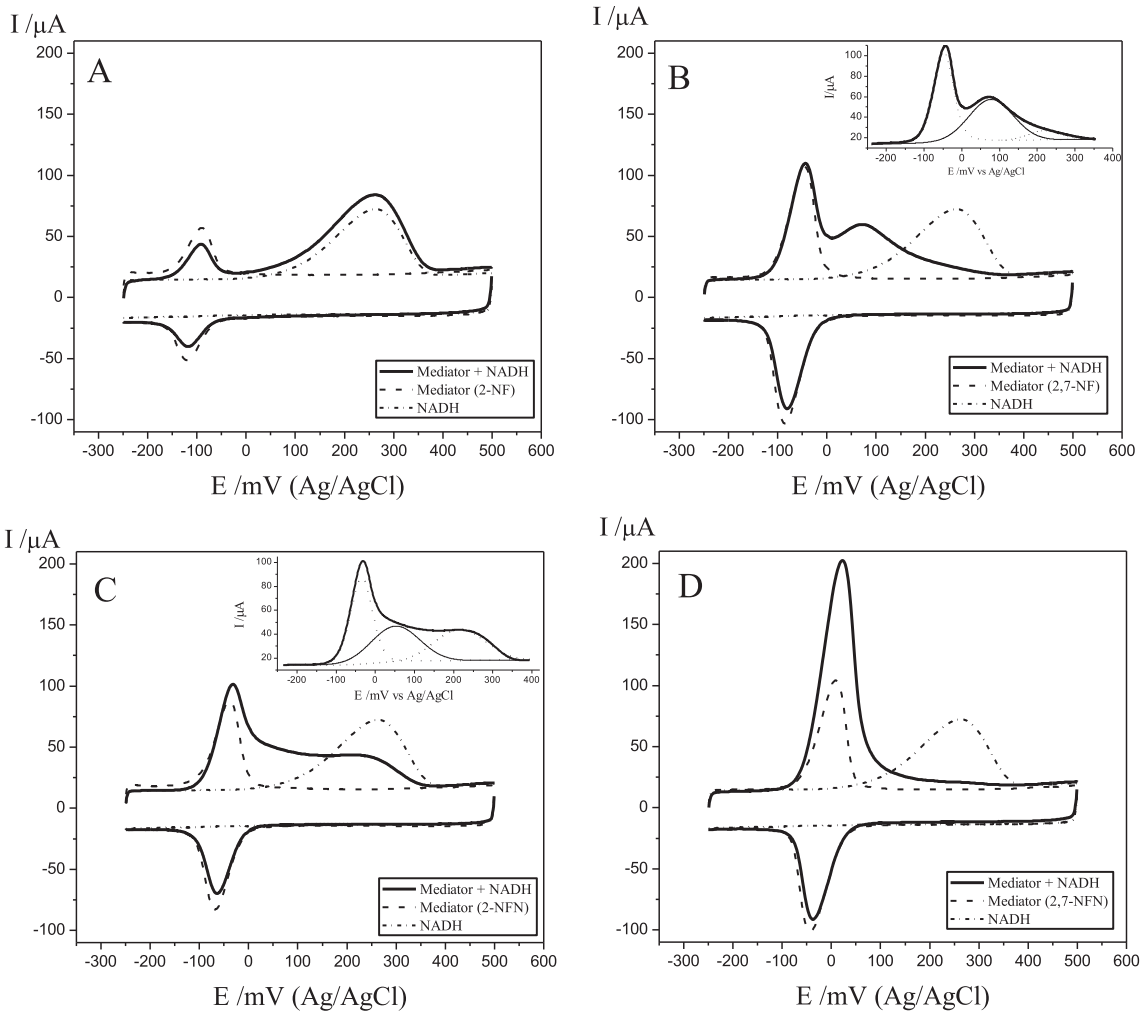

Fig. 6. Cyclic voltammograms in PBS buffer (0.1 M, pH 7.0) for MWCNT/GCE in a 0.2 mM NADH solution (dot-dashed line), mediator/MWCNT/GCE in a 0.2 mM NADH solution (solid line) and mediator/MWCNT/GCE (dashed line): (A) Mediator 2-NF, (B) 2,7-NF, (C) 2-NFN and (D)2,7-NFN when only one nitro group was reduced. Scan rate = 100 mV s^{-1}.

a single nitro group is reduced, the electrocatalytic activity of the redox mediator in the oxidation of NADH is determined by the substituents present in its molecular structure. Taking into account the effect of substituents, the observed catalytic effect is due to the reaction of the nitroso compound generated in the oxidation of hydroxylamine (reaction (2)) with NADH in solution that causes its oxidation:

$$R{-}NO - NADH + H^{+} \underset{k_{-1}}{\overset{k_1}{\rightleftarrows}} R - NHOH - NAD^{+} \quad (4)$$

Thus, in the presence of electro-acceptor substituents in the molecule, $k_1 \gg k_{-1}$, generating the hydroxylamine derivative that is oxidized again at this potential. This process ends when the NADH oxidation is completed. This is the case for the 2,7-NFN species which contains two electron-acceptor groups, and therefore a single oxidation peak for the hydroxylamine derivative generated in the processes described in Eqs. (2) and (4) is observed in the oxidation scan.

By contrast, 2-NF does not contain an electron-accepting group, so that $k_1 \ll k_{-1}$, and therefore no electrocatalytic effect is observed.

For the 2-NFN and 2,7-NF molecules, which contain only one electron-acceptor group (carbonyl and unreduced nitro, respectively), additional energy is necessary to oxidize the NADH, and it is observed that the oxidation of NADH occurs at potentials between that of hydroxylamine and that of NADH without a redox mediator.

4. Conclusions

The results demonstrate that 2,7-NFN/MWCNT/GCE shows both the lowest mediator redox couple potentials and the highest persistence at the electrode, giving rise to its enhanced electrocatalytic activity for NADH oxidation. The lowest mediator redox couple potential effect can be explained by the electronic effects of the nitro and C═O groups. On the other hand, the highest persistence at the electrode is a consequence of substitution by two nitro groups and one C═O group, which affects the π-π stacking interaction strength, allowing greater binding between the redox mediator and the nanostructured electrode platform.

Consequently, the nitro group has a triple effect: it acts as a precursor of the mediator redox couple for NADH electrocatalysis; enhances the π-π stacking interaction with the electrode; and also acts as an electron-acceptor substituent promoting the electrocatalysis of NADH.

Thus, modification of the substituents on a nitroaromatic compound trapped in the nanostructured platform makes it possible to tune the electrocatalytic effect of the nanostructured electrode platform.

CRediT authorship contribution statement

J. Urzúa: Methodology, Validation, Investigation, Data curation,

Writing - original draft. **C. Yañez:** Supervision, Software, Formal analysis, Writing - original draft, Writing - review & editing. **J. Carbajo:** Conceptualization, Supervision, Methodology, Validation, Investigation, Data curation, Writing - original draft. **J.D. Mozo:** Investigation, Data curation, Writing - original draft. **J.A. Squella:** Conceptualization, Methodology, Writing - original draft, Writing - review & editing, Supervision, Project administration, Funding acquisition.

Declaration of Competing Interest

The authors declare that they have no known competing financial interests or personal relationships that could have appeared to influence the work reported in this paper.

Acknowledgement

We thank FONDECYT Grant 1170054 and 1210899 for financial support.

Appendix A. Supplementary data

Supplementary data to this article can be found online at https://doi.org/10.1016/j.elecom.2020.106852.

References

[1] S. Ijima, Nature 354 (1991) 56–58, https://doi.org/10.1038/354056a0.
[2] A. Oberlin, M. Endo, T.J. Koyama, J. Cryst. Growth 32 (1976) 335–349, https://doi.org/10.1016/0022-0248(76)90115-9.
[3] M.A. Hamon, M.E. Itkis, S. Niyogi, T. Alvarez, C. Kuper, M. Menon, R.C. Haddon, J. Am. Chem. Soc. 123 (2001) 11292–11293, https://doi.org/10.1021/ja0109702.
[4] J. Han, Structures and properties of carbon nanotubes, in: M. Meyyappan (Ed.), Carbon Nanotubes: Science and Applications, CRC Press, London, 2005, p. 1.
[5] M. Pacios Pujadó, Carbon Nanotubes as Platforms for Biosensors with Electrochemical and Electronic Transduction, Springer, 2011, p. 9.
[6] G.G. Wildgoose, C.E. Banks, H.C. Leventis, R.G. Compton, Microchim. Acta 152 (2006) 187–214, https://doi.org/10.1007/s00604-005-0449-x.
[7] M. Liu, Y. Yang, T. Zhu, Z. Liu, Carbon 43 (2005) 1470–1478, https://doi.org/10.1016/j.carbon.2005.01.023.
[8] L. Zeng, L.B. Alemany, C.L. Edwards, A.R. Barron, Nano Res. 1 (2008) 72–88, https://doi.org/10.1007/s12274-008-8004-9.
[9] S. Shahrokhian, H.R. Zare-Mehrjardi, H. Khajehsharifi, J. Solid State Electrochem. 13 (2009) 1567–1575, https://doi.org/10.1007/s10008-008-0733-x.
[10] R.J. Chen, Y. Zhang, D. Wang, H. Dai, J. Am. Chem. Soc. 123 (2001) 3838–3839, https://doi.org/10.1021/ja010172b.
[11] L. Wang, S. Feng, J. Zhao, J. Zheng, Z. Wang, L. Li, Z. Zhu, Appl. Surf. Sci. 256 (2010) 6060–6064, https://doi.org/10.1016/j.apsusc.2010.03.120.
[12] C.G.R. Heald, G.G. Wildgoose, L. Jiang, T.G.J. Jones, R.G. Compton, Chemphyschem 5 (2004) 1794–1799, https://doi.org/10.1002/cphc.200400369.
[13] G.G. Wildgoose, S.J. Wilkins, G.R. Williams, R.R. France, D.L. Carnahan, L. Jiang, T.G.J. Jones, R.G. Compton, Chemphyschem 6 (2005) 352–362, https://doi.org/10.1002/cphc.200400403.
[14] M. Santhiago, P. Rodrigues Lima, W.J. Rodrigues Santos, A. Bof de Oliveira, L.T. Kubota, Electrochim. Acta 54 (2009) 6609–6616, https://doi.org/10.1016/j.electacta.2009.06.032.
[15] C.C. Correa, M. Santhiago, A.L. Barboza Formiga, L.T. Kubota, Electrochim. Acta 90 (2013) 309–316, https://doi.org/10.1016/j.electacta.2012.12.046.
[16] R. Moscoso, J. Carbajo, M. López, L.J. Núñez-Vergara, J.A. Squella, Electrochem. Commun. 13 (2011) 217–220, https://doi.org/10.1016/j.elecom.2010.12.027.
[17] R. Moscoso, J. Carbajo, J.A. Squella, J. Chil. Chem. Soc. 59 (2014) 2498–2501, https://doi.org/10.4067/S0717-97072014000200022.
[18] J. Urzúa, J. Carbajo, C. Yáñez, J.F. Marco, J.A. Squella, J. Solid State Electrochem. 20 (2016) 1131–1137, https://doi.org/10.1007/s10008-015-2949-x.
[19] R. Moscoso, J. Carbajo, J.D. Mozo, J.A. Squella, J. Electroanal. Chem. 765 (2016) 149–154, https://doi.org/10.1016/j.jelechem.2015.08.010.
[20] N. Mano, A. Kuhn, J. Electroanal. Chem. 477 (1999) 79–88, https://doi.org/10.1016/S0022-0728(99)00393-9.
[21] R. Moscoso, C. Barrientos, S. Moris, J.A. Squella, J. Electroanal. Chem. 837 (2019) 48–54, https://doi.org/10.1016/j.jelechem.2019.02.013.
[22] R. Moscoso, E. Inostroza, S. Bollo, J.A. Squella, Electrocatalysis 7 (2016) 357–361, https://doi.org/10.1007/s12678-016-0323-0.
[23] N. Mano, A. Thienpont, A. Kuhn, Electrochem. Commun. 3 (2001) 585–589, https://doi.org/10.1016/S1388-2481(01)00224-7.
[24] N. Mano, A. Kuhn, S. Menub, E.J. Dufourc, Phys. Chem. Chem. Phys. 5 (2003) 2082–2088, https://doi.org/10.1039/B212605B.
[25] L. Gorton, E. Domínguez, Rev. Mol. Biotech. 82 (2002) 371–392, https://doi.org/10.1016/S1389-0352(01)00053-8.
[26] T. Rębiś, M. Falkowski, G. Milczarek, T. Goslinski, ChemElectroChem 7 (2020) 2838–2850, https://doi.org/10.1002/celc.202000430.